

COMMISSIONING OF IFMIF PROTOTYPE ACCELERATOR TOWARDS CW OPERATION*

K. Masuda^{†1}, T. Akagi¹, A. De Franco¹, T. Ebisawa, K. Hasegawa, K. Hirosawa¹, J. Hyun, T. Itagaki, A. Kasugai, K. Kondo, K. Kumagai¹, S. Kwon¹, A. Mizuno², Y. Shimosaki³, M. Sugimoto¹,
 QST-Rokkasho, Aomori, Japan

P. Cara, Y. Carin¹, F. Cismondi¹, D. Duglué, H. Dzitko, D. Gex¹, A. Jokinen, I. Moya¹, G. Phillips,
 F. Scantamburlo¹, Fusion for Energy, Garching, Germany

N. Bazin, B. Bolzon, T. Chaminade, N. Chauvin, S. Chel, J. Marroncle, CEA Paris-Saclay, Gif sur
 Yvette, France

F. Arranz, B. Brañas, J. Castellanos, C. de la Morena, D. Gavela, D. Jimenez-Rey, Á. Marchena,
 P. Méndez, J. Molla, O. Nomen, C. Oliver, I. Podadera, D. Regidor, A. Ros, V. Villamayor, M. We-
 ber, CIEMAT, Madrid, Spain

L. Antoniazzi, L. Bellan, M. Comunian, A. Facco, E. Fagotti, F. Grespan, A. Palmieri, A. Pisent,
 INFN-LNL, Legnaro, Italy

¹also at IFMIF/EVEDA Project Team, Aomori, Japan

²also at JASRI/Spring-8, Hyogo, Japan

³also at KEK, Ibaraki, Japan

Abstract

A beam commissioning phase has started since July 2021 to pursue the world highest D⁺ beam current of 125 mA in CW at 5 MeV. Pilot beam operation as the first step with reduced beam currents of 10 mA H⁺ and 20 mA D⁺ identified needs of improvements in some newly installed components. The pilot beams were characterized, and comparisons were made with simulations for verification. CW commissioning of subsystems, namely injector, RFQ and RF power system, are being conducted in preparation to the nominal 125 mA D⁺ operation targeting CW.

INTRODUCTION

Construction of Linear IFMIF Prototype Accelerator (LIPAc) have been and are being conducted in Rokkasho, Aomori, Japan, within the EU-JA collaborative framework of the IFMIF/EVEDA project under the Broader Approach agreement [1]. The IFMIF, an accelerator-based D-Li neutron source, aims to provide highly intense neutron fluxes with appropriate energy spectrum in order to characterize materials for future fusion reactors. Because the IFMIF requires an accelerator with unprecedented performances to provide 40 MeV, 125 mA D⁺ beams in CW, the feasibility is being tested with a 1:1-scale prototype until the first cryomodule of the superconducting linac up to 9 MeV, namely the LIPAc. In this context, the LIPAc is to consist, in its final configuration in what is called the Phase C (see Fig. 1), of a 100 keV D⁺ beam Injector [2-4] incorporating an ECR ion source, the world longest RFQ [5-8] driven by eight 200 kW tetrode-based chains of RF power system (RFPS) at 175 MHz [9-10] to accelerate the beam up to 5

MeV, followed by a Medium Energy Beam Transport line (MEBT) [11] with highly space charged and beam loaded Buncher cavities [11,12], a superconducting RF (SRF) Linac, and a High Energy Beam Transport (HEBT) line [13] with a state-of-the-art Diagnostic Plate (D-Plate) [14,15], ending in a Beam Dump (BD) [16] designed to stop the world highest D⁺ current of 125 mA CW at 9 MeV.

A stepwise strategy as shown in Fig. 1 has been and will be applied to the installation and beam commissioning of the LIPAc [1]. The beam commissioning in the Phase B by temporary use of a Low Power Beam Dump (LPBD) has led to a successful acceleration of 125 mA D⁺ beam up to 5 MeV at the exit of RFQ in pulsed mode [17,18], without significant trace of unexpected beam loss [19]. Confirmation of the designed beam dynamics has been conducted successfully in terms of the beam transmission through the RFQ [20]. Following these milestones achieved in the

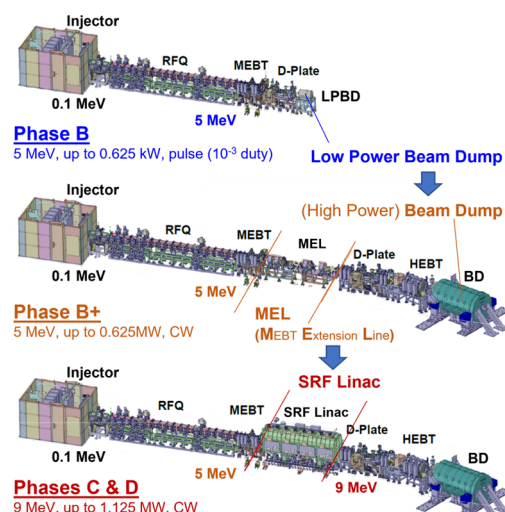


Figure 1: Three different layouts for the stepwise installation and commissioning of the LIPAc.

* This work was undertaken under the Broader Approach Agreement between the European Atomic Energy Community and the Government of Japan. The views and opinions expressed herein do not necessarily state or reflect those of the Parties to this Agreement.

[†] masuda.kai@qst.go.jp

Content from this work may be used under the terms of the CC BY 4.0 licence (© 2021). Any distribution of this work must maintain attribution to the author(s), title of the work, publisher, and DOI

earlier Phase B, the beam commissioning in the Phase B+ was initiated in July 2021 in a configuration where a beam transport line (MEBT Extension Line; MEL) [21] takes temporarily the position of the SRF linac.

The Phase B+ commissioning, which is on-going, aims at demonstrating an operation of 125 mA D⁺ beams at 5 MeV in CW. The characterization of the beam properties is also of major importance in preparation to the final configuration adding the SRF Linac, with a target normalized rms emittance of $0.25 \pi \text{ mm mrad}$. This paper aims to present the commissioning plan of the Phase B+ and the results that have been obtained so far.

COMMISSOING PLAN OF PHASE B+ TOWARDS CW

The major goals of the Phase B+ beam commissioning are, (1) to validate the Injector, RFQ and MEBT (including the Bunchers) up to CW with the nominal 125 mA D⁺ beam, (2) to validate the BD up to 0.625 MW CW (5 MeV instead of 9 MeV D⁺ beam), (3) to validate the beam diagnostics for both low and high duty operations, and (4) to characterize the beam properties to be injected into SRF linac in the following Phase C. Three stages of beam commissioning are planned in the Phase B+ as follows.

- **Stage 1** beam commissioning was conducted with H⁺ and then D⁺ beams of smaller currents than the nominal ones at low duty cycle (pilot beams, hereafter), for the purpose of tests and alignment checks of the newly installed components, as well as characterization of the pilot beams that are planned to be used also at the beginning of the Phase C.
- **Stage 2** aims at the nominal beam current of 125 mA D⁺ in pulsed mode with duty cycle less than 5 % for the purpose of characterization of the nominal D⁺ beam with applicability of interceptive diagnostics.
- **Stage 3** will then follow the Stage 2, targeting the CW operation of 125 mA D+ beams by utilizing non-interceptive diagnostics.

Since completion of the Stage 1 in December 2021, a CW beam commissioning of the Injector has been conducted. In parallel, RF conditioning of the RFQ up to CW are being pursued. The results from the Stage 1 as well as the status of the Injector and RFQ CW campaigns will be presented in the following chapters. The Stage 2 is planned to start in the spring of 2023 after completion of the CW campaigns.

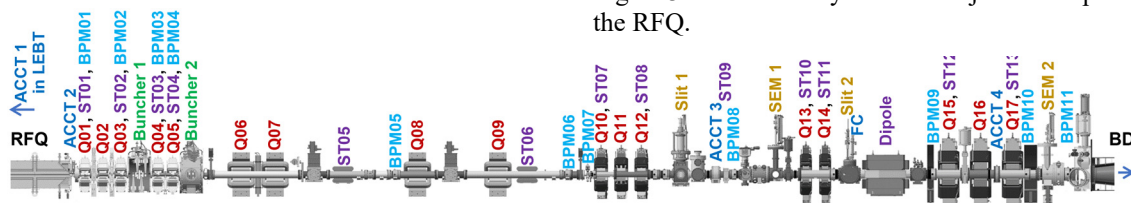


Figure 2: Layout of components along the beamline from the RFQ exit to the BD. Dipole, Q01-17 and ST01-13 denotes a bending, quadrupole and steering magnets, respectively, FC, a Faraday cup, and SEMs, beam profile monitors based on secondary electron emission grids. Some non-interceptive diagnostics are not shown for simplicity.

BEAM COMMISSIONING STAGE 1 WITH LOW CURRENT H⁺ AND D⁺ BEAMS

The Stage 1 beam commissioning was initiated in July 2021. It was resumed after a 3-month break mainly for a scheduled summer maintenance and was completed in December 2021 with a total duration of around 7 weeks.

Injector Operation

The pilot beams are meant to start up the beam commissioning in the Phase B+ (namely the Stage 1) as well as at the beginning of the Phase C after installing the SRF Linac with minimal beam losses before and during tuning of the magnets along the beamline (see Fig. 2).

A low D⁺ beam current of ~20 mA (in macro-pulse peak) at the exit of RFQ was targeted, which was expected and eventually confirmed in the Stage 1 to be visible in all the BPMs located along the beamline down to the BD when the Bunchers are used. A half current, i.e. ~10 mA, was targeted for the H⁺ pilot beam for the use prior to the D⁺ pilot beam at half beam energies (50 keV at the LEBT and 2.5 MeV at the RFQ exit) with the same perveance as the D+ pilot beam. These target beam currents were accomplished by use of a plasma electrode (PE, see Fig. 3) with an extraction aperture of 6 mm ϕ , and by tuning the ECR power and the intermediate electrode bias while the solenoid and steering magnets (SOLs and STs in Fig. 3) were tuned to maximize the beam transmission to the RFQ exit by monitoring the ACCT 2 placed there in the MEBT.

As for the duty cycle for the pilot beams, the pulse width and repetition rate in the present Stage 1 were 100 μsec and 1 Hz, respectively, except for a few Hz and/or several hundreds μsec in order for better statistics in beam property measurements. A shorter width of 60 μsec was also tested in preparation to the Stage 2 in order to avoid damages of the SEMs anticipated by the nominal 125 mA D+ beams in some cases when focused onto them. The pulsing of the beam was accomplished by use of the chopper successfully as seen in Fig. 4 for the 20 mA D⁺ pilot beams. In a high contrast, a significant delay at the rising edge of the chopper gate was observed in the 10 mA H⁺ case, with transient ACCT waveforms lasting over the 100 μsec pulse width. A

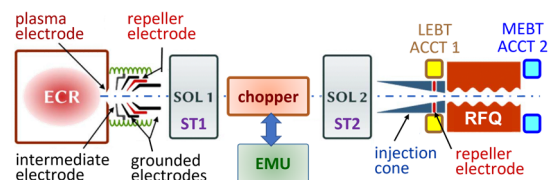


Figure 3: Schematic layout of the Injector components and the RFQ.

Kr gas was then injected to enhance the space charge compensation (SCC) in the LEBT, which turned out to reduce the transient time duration in ACCTs down to $\sim 20 \mu\text{sec}$ at the expense of $\sim 10\%$ degradation in the beam current at the plateau (i.e. the macro-pulse peak). More details will be presented in a paper published later.

Beam Transport and Alignment Check

Beam-based alignment of the pilot beams to some selected quadrupoles (Qs in Fig. 2) were carried out one by one from upstream, to each Q by tuning a steering magnet (ST) upstream and a BPM downstream to monitor the beam center displacement while the Q was scanned [22]. All the Qs were then scanned to determine the beam positions with respect to the magnetic centers of the Qs similarly by the beam-based technique. As the result the D^+ pilot beam centers were confirmed to be within $\pm 0.2 \text{ mm}$ in horizontal and vertical of the Qs with a couple of exceptions [22].

The envisaged next step of beam-based calibration of the BPM signal ratios (determination of the BPM centers) was postponed to the Stage 2 after works on issues identified in the Stage 1 related to acquisition circuits, and RF noise at 175 MHz originating probably from the RFPS [23].

Meanwhile, for the purpose of alignment checks of the Qs, relative positions among the Qs were evaluated from the determined steering angles in the STs and the beam positions with respect to the magnetic centers of the Qs. An example of successful application of this scheme is shown in Fig. 5, where a 0.5 mm misalignment between the RFQ exit and Q01 found earlier by use of a laser-tracker is seen reproduced by the beam-based scheme, assuming the beam passing through the center of the RFQ exit [22].

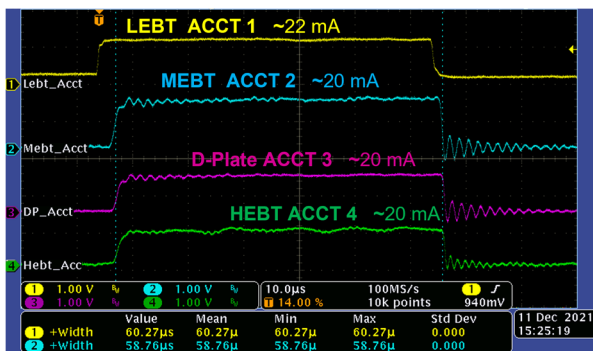


Figure 4: Current transformer waveforms by the ACCTs 1 to 4 depicted in Figs. 1 and 2, with a 60 μsec pulse width (chopper gate) and $\sim 20 \text{ mA}$ D^+ current at the RFQ exit.

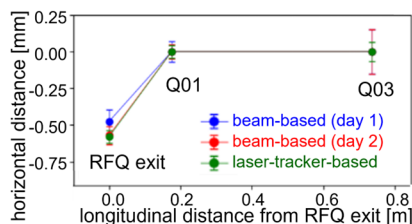


Figure 5: Alignment survey results, comparing between laser-tracker-based and beam-based ones [22].

Beam Characterization and Comparison with Simulations

Characterization of the pilot beams were performed. Horizontal (x) and vertical (y) profiles were obtained by use of the Slit 1 (see Fig. 2) in combination with the ACCT 3 as well as by use of the SEMs 1 and 2. In addition, the Slit 2, a horizontal beam slit, was used in combination with the FC to obtain a y-profile of a beam already cut by the Slit 1, a vertical slit. Either horizontal or vertical phase space ($x-x'$ or $y-y'$) profiles at the position of the Slit 1 were obtained in combination with SEM 1 and ST09. As seen in Figs. 6(a) and (b) for example, x- and y-profiles by the Slits were seen fit well with Gaussian, compared with those by the SEMs in Figs. 6(c) and (d). To check uniformity in wire gains, the beam was scanned over the SEMs by use of STs upstream, resulting in different x-profiles indicated by x_1 to x_4 in Figs. 6(c) and (d). A clear difference was seen in the beam sizes by the Gaussian fitting especially between x_1 and x_2 in Fig. 6(c), implying need of gain calibration over the SEM wires, though not applied yet to the measured beam properties presented in this paper.

Figure 7 and Table 1 compare the measured profiles of the 20 mA D^+ pilot beams with simulations in three cases with different settings of Q11 and Buncher 1. The simulations were carried out by use of TraceWin and Toutatis codes[24], starting at the position of the EMU in the Injector (see Fig. 3) by use of a $y-y'$ profile measured by the EMU (Alison scanner) and on an assumption of cylindrical symmetry. Instead of use of PIC-MC simulations [25,26] or semi-analytical model [26] well developed earlier, a uniform SCC degree (SCCD) was assumed between the EMU and the RFQ entrance in this study, though a strong longitudinal dependence is known [26]. The SCCD averaged over the distance, so to say, was then determined so that the numerical dependence of beam transmission to the RFQ exit on the SOL2 current agrees to the experimental one. Simulations were performed for this purpose assuming different SCCDs from 50 to 95 % with a 5 % step. As the result those with 50% and 70 % (and higher) were rejected, and thus those with 55 and 65 % SCCDs are summarized in Table 1 and the one with 60 % is illustrated in Fig. 7.

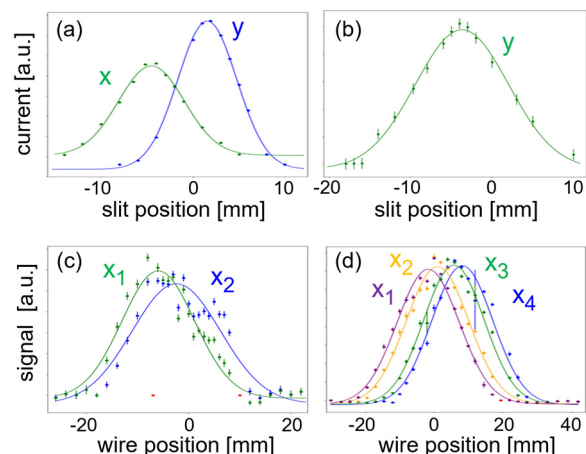


Figure 6: Examples of transverse beam profiles measure at (a) Slit 1, (b) Slit 2, (c) SEM 1 and (d) SEM 2.

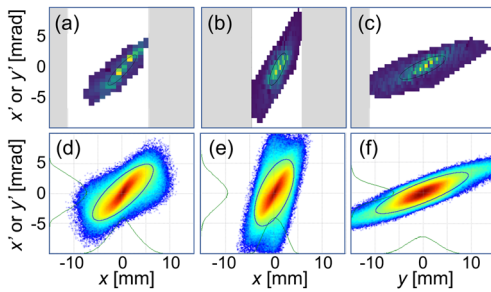


Figure 7: Transverse phase space profiles at Slit 1 in the 3 cases (left, middle and right), comparing measurements (top) and simulations (bottom). White and grey backgrounds in top images indicate measurement windows.

Table 1: Beam Properties by Measurements with 1σ Errors (above), and Simulations with 55 – 65 % SCCD (below). Blue color indicates agreement within 1σ measurement error, green within 2σ , purple within 3σ and red beyond 3σ .

	case 1	case 2	case 3
Q11	97 A	127 A	97 A
Buncher 1	200 kV at bunching phase	200 kV at bunching phase	0 kV
$-\alpha$	1.47 ± 0.92 1.16 – 1.37	1.21 ± 0.15 0.71 – 0.87	1.30 ± 0.43 1.82 – 1.59
γ / β	0.81 ± 0.48 0.54 – 0.62	2.39 ± 0.38 2.05 – 1.76	0.17 ± 0.06 0.12 – 0.12
ϵ_n	0.42 ± 0.24 0.29 – 0.26	0.23 ± 0.03 0.29 – 0.25	0.44 ± 0.14 0.28 – 0.23
	Slit 1	SEM 1	SEM 2
case 1, σ_x	3.0 ± 0.1 2.9 – 2.7	7.5 ± 0.1 5.8 – 5.8	8.4 ± 0.1 6.5 – 6.5
case 1, σ_y	3.7 ± 0.1 4.3 – 3.8	9.0 ± 0.1 6.4 – 5.8	3.7 ± 0.1 2.5 – 2.4
case 2, σ_x	1.8 ± 0.1 1.8 – 1.8	n/a	n/a
case 3, σ_y	4.8 ± 0.3 4.8 – 4.1	n/a	n/a

Agreements within the SCCD uncertainty in simulations and within 2σ statistical errors in measurements are seen except for α in the case 2, and the beam sizes by the SEMs, to which the SEM wire gain variations might contribute. It should be noted that the measured Twiss parameters and emittances might also be affected.

RF CONDITIONING OF RFQ

Following the achievement of the nominal RFQ vane voltage in pulsed mode in the earlier Phase B [17,18], RF conditioning of the RFQ to reach CW has been pursued. The RF conditioning performed in the night shift, in parallel to the Stage 1 beam commissioning in the daytime, suffered from interlock events limiting the duty cycle at $\sim 25\%$ until (A) in Fig. 8. We then changed our strategy to reach CW first at a reduced RFQ voltage and then to increase the voltage, which led to a successful achievement of reaching CW at 80 % of the nominal RFQ voltage at (B) in Fig. 8.

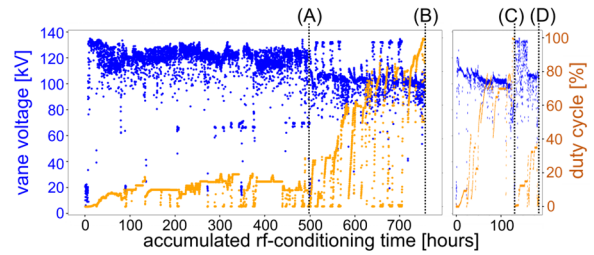


Figure 8: RFQ voltage and duty cycle histories during RF conditioning of the RFQ.

After a winter break, the RF conditioning was resumed to aim at the nominal RFQ voltage in CW, where we met major troubles; a circulator in the RFPS was found damaged at (C) in Fig. 8, and during the RF conditioning by use of the rest seven chains a vacuum leak was detected at (D), which eventually revealed Viton O-rings in five of the eight RF couplers were deformed due to overheat. Following analyses of these two events, recovery works are being conducted to resume the RF conditioning in early 2023.

INJECTOR CW BEAM COMMISSIONING

In parallel to the RFQ RF conditioning, CW beam commissioning of the Injector is being conducted to obtain stably operational currents and emittances with different extraction apertures (Fig. 9). Figure 10 shows an example of CW long runs in the case marked by red dotted circle in Fig. 9, where a total extracted current of 150 mA including molecular ions, and a normalized rms emittance of 0.27π mm mrad have been obtained by use of 11 mm ϕ PE. A CW run of more than 11 hours has been reached in this case. Conditioning is to be performed to reduce the trip rate further once the PE aperture for the Stage 2 operation is determined. Targeting a total extracted current of ~ 160 mA, a larger PE of 12 mm ϕ is being tested, and a couple of PEs of intermediate apertures are prepared for tests if needed.

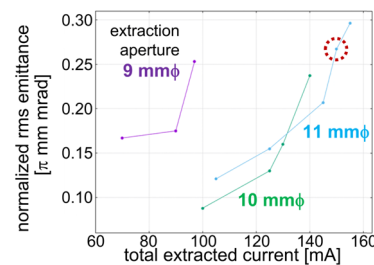


Figure 9: Stably operational emittance (at 5% duty cycle) and total extracted current with different PE apertures.

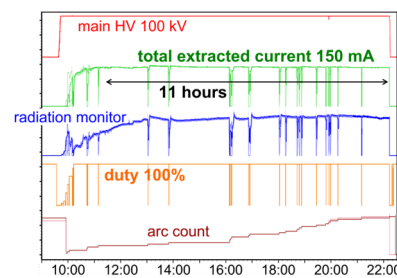


Figure 10: A CW long run with a 11mm ϕ PE.

CONCLUSION

The Stage 1 beam commissioning was completed in December 2021. The injector was tuned to produce the so-called pilot beams, namely H⁺ and D⁺ beams of as low currents as 10 mA and 20 mA respectively, for the purposes of a safe start-up of beam commissioning in the Phase B+ as well as in the Phase C after installing the SRF Linac. The pilot beams were transported down to the Beam Dump successfully without significant beam loss, and the beam characterisation was carried out with satisfactory agreement with the simulations. The newly installed components for the Phase B+ were mostly checked and validated by the use of the pilot beams, while some needs of improvements to be coped with before the following stages were identified.

In preparation to the following stages which aim at the nominal current of 125 mA D⁺ CW, RF conditioning of the RFQ up to CW is being pursued. So far, 25 % duty at the nominal vane voltage and 100 % duty (CW) at a reduced voltage have been reached. In parallel, CW beam commissioning of the Injector is being conducted with different extraction apertures. A successful CW operation has been reached so far with a total extracted current of 150 mA including molecular ions, and a normalized rms emittance of 0.27 π mm mrad. A target total extracted current of 160 mA with a smaller emittance is being pursued.

REFERENCES

- [1] H. Dzitko *et al.*, “Status and future developments of the Linear IFMIF Prototype Accelerator (LIPAc)”, *Fusion Eng. Des.*, vol. 168, p. 112621, Jul. 2021. doi:10.1016/j.fusengdes.2021.112621
- [2] R. Gobin *et al.*, “Final design of the IFMIF injector at CEA/Saclay”, in *Proc. IPAC’13*, Shanghai, China, Jun. 2013, pp. 3758-3760.
- [3] N. Chauvin *et al.*, “Deuteron beam commissioning of the linear IFMIF prototype accelerator ion source and low energy beam transport”, *Nucl. Fusion*, vol. 59, no. 10, p. 106001, Aug. 2019. doi:10.1088/1741-4326/ab1c88
- [4] T. Akagi *et al.*, “Commissioning of high current H⁺/D⁺ ion beams for the prototype accelerator of the International Fusion Materials Irradiation Facility”, *Rev. Sci. Instr.*, vol. 91, no. 2, p. 023321, Feb. 2020. doi:10.1063/1.5129598
- [5] A. Piesent *et al.*, “IFMIF-EVEDA RFQ design”, in *Proc. EPAC’08*, Genoa, Italy, Jul. 2008, pp. 3542-3544.
- [6] F. Grespan *et al.*, “RF design of the IFMIF-EVEDA RFQ”, in *Proc. LINAC’08*, Victoria, BC, Canada, Sep.-Oct. 2008, pp. 148-150.
- [7] M. Communian *et al.*, “Beam dynamics of the IFMIF-EVEDA RFQ”, in *Proc. EPAC’08*, Genoa, Italy, Jul. 2008, pp. 3536-3538.
- [8] M. Communian *et al.*, “The IFMIF-EVEDA RFQ: Beam dynamics design”, in *Proc. LINAC’08*, Victoria, BC, Canada, Sep.-Oct. 2008, pp. 145-147.
- [9] P. Mendez *et al.*, “LIPAc RF power system: design and main practical implementation issues”, *Fusion Eng. Des.*, vol. 165, p. 112226, Apr. 2021. doi:10.1016/j.fusengdes.2021.112226
- [10] M. Weber *et al.*, “Functional overview of the rf power system for the LIPAc RFQ”, *IEEE Trans. Plasma Sci.*, vol. 49,

- no. 9, pp. 2987-2996, Aug. 2021. doi:10.1109/TPS.2021.3102840
- [11] I. Podadera *et al.*, “The medium energy beam transport line (MEBT) of IFMIF/EVEDA LIPAc”, in *Proc. IPAC’11*, San Sebastián, Spain, Sep. 2011, pp. 2628-2630.
- [12] D. Gavela *et al.*, “Validation of two re-buncher cavities under high beam loading for LIPAc”, in *Proc. IPAC’21*, Campinas, SP, Brazil, May 2021, pp. 4343-4345. doi:10.18429/JACoW-IPAC2021-THPAB272
- [14] I. Podadera *et al.*, “A diagnostics plate for the IFMIF-EVEDA accelerator”, in *Proc. EPAC’08*, Genoa, Italy, Jul. 2008, pp. 1248-1250.
- [15] J. Marroncle *et al.*, “IFMIF-LIPAc diagnostics and its challenges”, in *Proc. IBIC’12*, Tsukuba, Japan, Oct. 2012, pp. 557-565.
- [13] B. Brañas *et al.*, “Design, manufacturing and tests of the LIPAc high energy beam transport line”, *Nucl. Fusion*, vol. 61, p. 015001, Nov. 2021. doi:10.1088/1741-4326/abbba1
- [16] B. Brañas *et al.*, “IFMIF-EVEDA accelerator: Beam dump design”, in *Proc. EPAC08*, Genoa, Italy, Jul. 2008, pp. 1248-1250.
- [17] K. Kondo *et al.*, “Validation of the Linear IFMIF Prototype Accelerator (LIPAc) in Rokkasho”, *Fusion Eng. Des.*, vol. 153, p. 111503, Feb. 2020. doi:10.1016/j.fusengdes.2020.111503
- [18] F. Grespan *et al.*, “IFMIF/EVEDA RFQ beam commissioning at nominal 125 mA deuteron beam in pulsed mode”, in *Proc. IPAC’20*, Caen, France, May 2020, pp. 21-25. doi:10.18429/JACoW-IPAC2020-TUVIR11
- [19] K. Kondo *et al.*, “Neutron production measurement in the 125 mA 5 MeV deuteron beam commissioning of Linear IFMIF Prototype Accelerator (LIPAc) RFQ”, *Nucl. Fusion*, vol. 61, no. 11, p. 116002, Sep. 2021. doi:10.1088/1741-4326/ac233c
- [20] L. Bellan *et al.*, “Acceleration of the high current deuteron beam through the IFMIF-EVEDA RFQ: confirmation of the designed beam dynamics performances”, in *Proc. HB’21*, Batavia, IL, USA, Oct. 2021, pp. 197-202. doi:10.18429/JACoW-HB2021-WEDC2
- [21] Y. Shimosaki *et al.*, “Lattice Design for 5MeV-125mA CW RFQ Operation in LIPAc”, in *Proc. IPAC’19*, Melbourne, VIC, Australia, May 2019, pp. 977-979. doi:10.18429/JACoW-IPAC2019-M0PTS051
- [22] J. Hyun *et al.*, “Evaluation of quadrupole misalignment in the IFMIF prototype accelerator using the beam based-alignment method”, submitted for publication.
- [23] K. Hirose *et al.*, “Beam test and the present status of beam position and phase monitor in the LIPAc Phase-B+ commissioning”, submitted for publication.
- [24] DACM Software for Accelerator Design and Simulation, <https://dacm-logiciels.fr/>
- [25] N. Chauvin *et al.*, “Beam dynamics simulation of the low energy beam transport line for IFMIF/EVEDA”, in *Proc. LINAC’08*, Victoria, BC, Canada, Sep.-Oct. 2008, pp. 242-244.
- [26] L. Bellan *et al.*, “Extraction and low energy beam transport models used for IFMIF/EVEDA RFQ commissioning”, *J. Phys.: Conf. Ser.*, vol. 2244, p. 012078, 2022. doi:10.1088/1742-6596/2244/1/012078